Genetic Evidence That Cellulose Synthase Activity Influences Microtubule Cortical Array Organization[1][W][OA]

Alexander R. Paredez, Staffan Persson, David W. Ehrhardt, and Chris R. Somerville*

Department of Plant Biology, Carnegie Institution, Stanford, California 94305 (A.R.P., D.W.E., C.R.S.); Department of Molecular and Cell Biology, University of California, Berkeley, California 94720 (A.R.P.); Department of Biological Sciences, Stanford University, Stanford, California 94305 (A.R.P., C.R.S.); and Max-Planck-Institut für Molekulare Pflanzenphysiologie, 14476 Golm, Germany (S.P.)

To identify factors that influence cytoskeletal organization we screened for Arabidopsis (*Arabidopsis thaliana*) mutants that show hypersensitivity to the microtubule destabilizing drug oryzalin. We cloned the genes corresponding to two of the 131 mutant lines obtained. The genes encoded mutant alleles of *PROCUSTE1* and *KORRIGAN*, which both encode proteins that have previously been implicated in cellulose synthesis. Analysis of microtubules in the mutants revealed that both mutants have altered orientation of root cortical microtubules. Similarly, isoxaben, an inhibitor of cellulose synthesis, also altered the orientation of cortical microtubules while exogenous cellulose degradation did not. Thus, our results substantiate that proteins involved in cell wall biosynthesis influence cytoskeletal organization and indicate that this influence on cortical microtubule stability and orientation is correlated with cellulose synthesis rather than the integrity of the cell wall.

Before cortical microtubules were first observed, their existence and function in plant morphogenesis was hypothesized by Green (1962), who treated algal cells with the antispindle drug colchicine and observed a change in the orientation of cellulose microfibril deposition (Green, 1962). Soon after, Ledbetter and Porter (1963) published the first electron microscopy images of plant cell spindle fibers and observed similar fibers at the cell cortex, all with the same hollow structure that they subsequently renamed microtubules. Importantly, these images showed that microtubules were oriented parallel to cellulose microfibrils, and the idea that microtubules might guide cellulose deposition, termed the alignment hypothesis, was introduced (Green, 1963; Ledbetter and Porter, 1963). This idea became controversial as conflicting studies were published over the last four decades (for review, see Baskin, 2001). However, recent live-cell imaging of the spatial and temporal relationship between the cellulose synthase (CESA) complex and cortical microtubules in Arabidopsis hypocotyl cells provided compelling evidence in support of the alignment hypothesis (Paredez et al., 2006).

Although a role for cortical microtubule guidance of the CESA complex has been controversial, the importance of the cortical microtubule array in plant morphogenesis is well documented. Depolymerization of microtubules using inhibitors, the knockdown, or the temperature-sensitive XMAP215, *mor1* mutant results in iso-diametric cell swelling (Green, 1962; Baskin et al., 1994; Sugimoto et al., 2000; Bao et al., 2001; Whittington et al., 2001). Furthermore, several morphogenic mutants have been identified, with subtle to extreme microtubule phenotypes, in which the morphology defects correspond to the level of microtubule disorganization. For example, point mutations affecting tubulins TUA4 and TUA6 (*lefty1* and *lefty2*, respectively) result in obliquely oriented cortical arrays, twisting of the stem and root axes, and roots that grow with a left-handed skew (Thitamadee et al., 2002). In addition, mutations in the *pilz* group of genes, encoding tubulin folding cofactors, result in embryo lethality (Steinborn et al., 2002). Between the extremes of axial twisting and lethality is *botero1*, which carries a mutation in the p60 subunit of katanin (Bichet et al., 2001; Burk et al., 2001). The cortical arrays of the *botero1* mutant are severely disorganized and, as a result, its cells are short and swollen (Bichet et al., 2001).

In the rapidly expanding cells of roots and dark-grown hypocotyls, microtubules remain roughly transverse until cells approach their maximal length (Sugimoto et al., 2000; Le et al., 2005). Transverse microtubule arrays guide cellulose deposition and are required for anisotropic cell expansion, such that the major axis of growth is parallel to the long axis of the

[1] This work was supported by a grant from the U.S. Department of Energy (DOE–FG02–03ER20133). S.P. was funded by the Max-Planck Gesellschaft.

* Corresponding author; e-mail crs@berkeley.edu.

The author responsible for distribution of materials integral to the findings presented in this article in accordance with the policy described in the Instructions for Authors (www.plantphysiol.org) is: Chris R. Somerville (crs@berkeley.edu).

[W] The online version of this article contains Web-only data.

[OA] Open Access articles can be viewed online without a subscription.

www.plantphysiol.org/cgi/doi/10.1104/pp.108.120196

organelle. In roots, the orientation of the cortical arrays correlates with developmental position. Arrays are transversely orientated where epidermal cells emerge from under the root cap marking the beginning of the elongation zone. The cortical arrays of cells remain transverse as cells move through the elongation zone, with some cells displaying obliquely oriented cortical arrays just before root hair emergence, which marks the point where elongation slows (Dolan et al., 1994; Sugimoto et al., 2000; Baskin et al., 2004). Shortly after root hair emergence, cell elongation ceases and the microtubules become longitudinally oriented.

The arrays of dark-grown hypocotyls differ from roots in that they respond to both developmental position and light (Le et al., 2005; Paredez et al., 2006). Light induces rapid transitions of cortical microtubules, within 5 to 10 min, from transverse to longitudinal orientation being possible (Paredez et al., 2006). In contrast to the fixed orientation of the array in rapidly expanding cells, the cortical arrays of light grown hypocotyls have been observed to undergo constant steady rotations requiring 200 to 800 min to rotate through 360° (Chan et al., 2007). In addition to light and developmental position, hormones have also been shown to affect cortical array orientation (Shibaoka, 1994).

The mechanism by which cortical arrays become organized and oriented with respect to the plant organ axis remains unclear. A key feature of cortical microtubules is their association with the cell cortex. The proteins responsible for maintaining this association remain largely unidentified; however, this property is important as it signifies that order need only be established in two dimensions. This process has been speculated to involve largely microtubule treadmilling and bundling (Wasteneys, 2002; Shaw et al., 2003; Dixit and Cyr, 2004; Ehrhardt, 2008). It is understood that tubulin dynamicity and stability are affected by microtubule-associated proteins that can have a profound effect on cortical microtubule organization. For example, overexpression of MAP18, a microtubule destabilizing factor, causes cortical arrays to become longitudinally orientated (Wang et al., 2007). Deletion of katanin results in the disordered cortical arrays of *botero*, while overexpression leads to the formation of unusually thick bundles that subsequently give way to fragmented cortical arrays (Bichet et al., 2001; Stoppin-Mellet et al., 2006). It is evident that a balance between stabilization and destabilization is required to allow for normal cortical array organization and organ morphogenesis. It is thought that the cortical array must constantly shift so that cellulose is properly spooled along the cell axis. Stabilization of cortical arrays with taxol results in cell swelling, indicating the presence of intact cortical arrays is not sufficient for proper morphogenesis (Baskin et al., 1994).

To further the understanding of the plant cytoskeleton, and its effects on morphogenesis, additional cytoskeletal components and regulators need to be identified. Hypersensitive drug screens have successfully been used to identify mutants that are directly associated with the drug targets (Stearns et al., 1990; Giaever et al., 1999; Naoi and Hashimoto, 2004). Therefore, we used threshold concentrations of oryzalin, a potent plant herbicide that functions by sequestering tubulin dimers (Hugdahl and Morejohn, 1993), to screen for Arabidopsis mutants with altered assembly of the tubulin cytoskeleton. We identified 131 oryzalin-hypersensitive mutant lines and characterized two of these mutants, both of which have a role in cellulose synthesis. We interpret the phenotypes of these mutants as evidence that the CESA complexes or their activity influences cortical microtubule array stability and organization. Thus, while cortical array organization directs the trajectories of CESA complexes (Paredez et al., 2006), the result of their activity affects cortical array organization.

RESULTS

Screen for Increased Oryzalin Sensitivity

To identify factors that may affect microtubule organization we screened ethyl methanesulfonate (EMS) mutagenized Arabidopsis seedlings for increased sensitivity to the microtubule-destabilizing drug oryzalin. The threshold concentration of the drug was determined by germinating Arabidopsis wild-type seedlings on plates containing 50 to 800 nM oryzalin. Similar to previous studies, a threshold for wild-type sensitivity was determined to be near 175 nM oryzalin (Baskin et al., 1994). Approximately 50,000 EMS-mutagenized seedlings were screened by transferring 4-d-old seedlings to media containing oryzalin and scoring for root swelling. Seedlings with root swelling were rescued and their progeny retested. Our collection contains 131 mutant lines with increased sensitivity to oryzalin. Two of the mutants, lines 16-2 and 52-isx, were selected for further analyses. Both 16-2 and 52-isx exhibited moderate sensitivity to oryzalin compared to other mutants in the collection (Figs. 1, A–I, and 2D). However, both mutants also displayed additional phenotypes reminiscent of cellulose-deficient mutants (Fig. 2, A and C), suggesting that the affected genes may present links between the cortical microtubules and the plant cell wall. The 16-2 seedlings exhibited short swollen roots and reduced etiolated hypocotyl lengths when grown at standard temperatures (22°C; Fig. 2, A and B). However, this phenotype was suppressed when seedlings were grown at 29°C (Supplemental Fig. S1), and 16-2 seedlings were also less sensitive to oryzalin at this temperature (data not shown). The 52-isx seedlings exhibited short, radially swollen, etiolated hypocotyls (Fig. 2A), and increased sensitivity to the CESA inhibitor isoxaben (Fig. 2C). Root diameter measurements of seedlings grown on media containing 175 nM oryzalin showed that 16-2 and 52-isx roots were significantly wider (16.4% and 17.6%, respectively) compared to wild-type (4.5%) roots (Fig. 3). When seedlings were transferred from control media

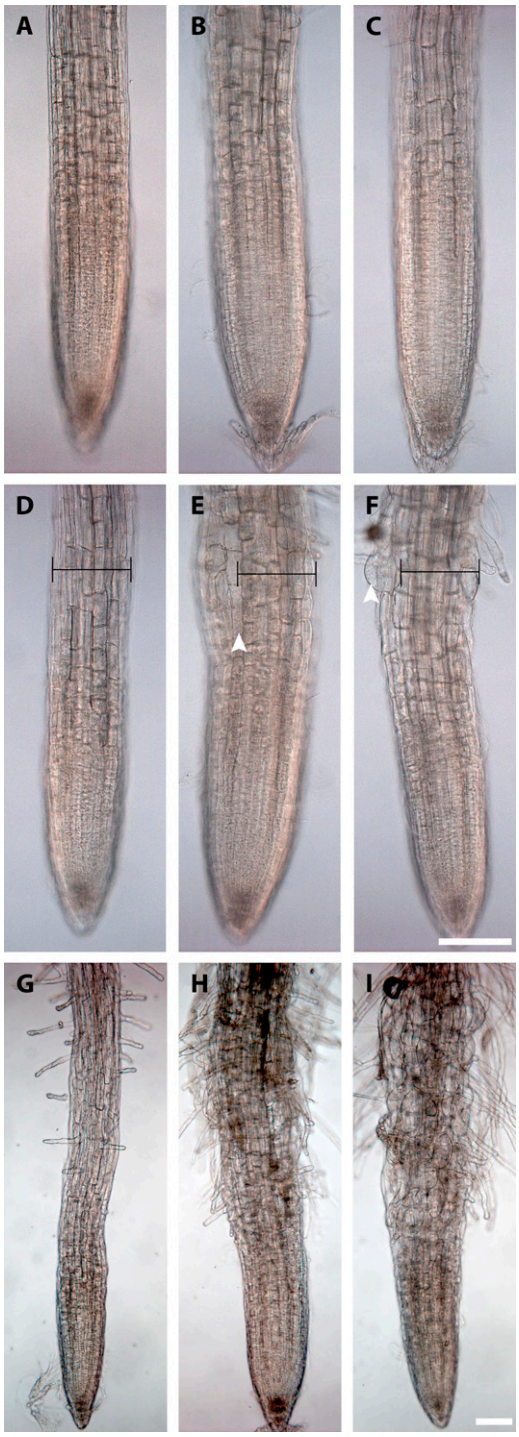

Figure 1. Root phenotypes of oryzalin-hypersensitive mutants 16-2 and 52-isx. A to I, Ecoptype Columbia of Arabidopsis (Col-0; A, D, and G); 16-2 (B, E, and H); and 52-isx (C, F, and I). A to C, Roots of 5-d-old seedlings grown on MS media containing 0.017% methanol. D to F, Roots of 5-d-old seedlings grown on MS containing 175 nM oryzalin. Col-0 (A and D) does not exhibit apparent cell swelling when grown on 175 nM oryzalin while line 16-2 (B and E) and 52-isx (C and F) exhibited swollen cells when grown in the presence of oryzalin. G to I, Roots of 7-d-old seedlings first grown on MS media for 4 d and then transferred to 175 nM oryzalin plates for three additional days exhibit more severe swelling. Caliper bar in D to F is set to the width of Col-0 root in D. Scale bar = 100 μm.

to media containing 175 nM oryzalin root swelling was more apparent (Figs. 1, G–I, 2E, and 3). The root diameter of 52-isx increased by 64% while, the wild type and 16-2 had similar increases of 30%. Interestingly, root lengths were reduced proportionally (30% length reduction) for all lines grown on 175 nM oryzalin (data not shown).

Microtubule Organization Defects in 16-2 and 52-isx

Cortical microtubule organization in Arabidopsis roots is stereotyped and highly ordered in rapidly expanding cells (Sugimoto et al., 2000). To assess whether this order was maintained in 16-2 and 52-isx seedlings we generated reciprocal crosses between the mutants and a GFP-MAP4 marker line that facilitates visualization of microtubules in live root cells (Marc et al., 1998). Cells in the early elongation zone of the root harbored densely packed cortical arrays with a strong transverse organization (Fig. 4A). In older but still elongating cells the spacing between the elements

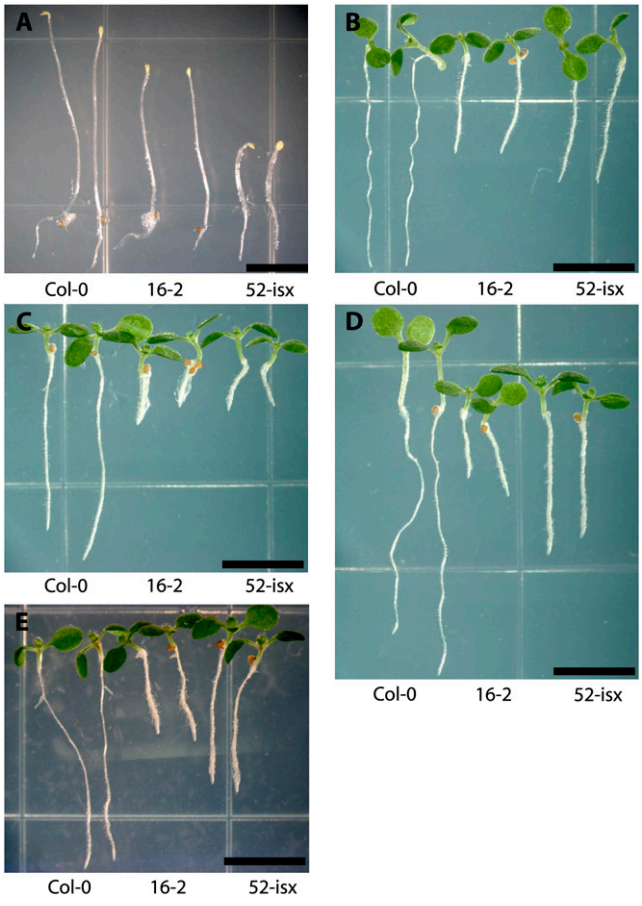

Figure 2. Seedling phenotypes of 16-2 and 52-isx mutants. A, Five-day-old etiolated Col-0, 16-2, and 52-isx seedlings. B to D, Five-day-old Col-0, 16-2, and 52-isx seedlings grown under 24-h light on MS media (B), 1.5 nM isoxaben (C), and 175 nM oryzalin (D). E, Col-0, 16-2, and 52-isx seedlings were grown on MS media for 4 d and then transferred to 175 nM oryzalin for another 3 d. Scale bar = 5 mm.

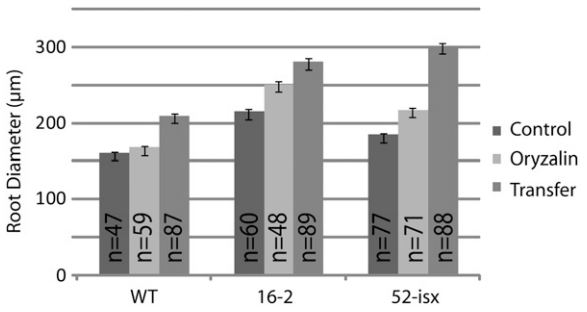

Figure 3. Measurement of root swelling in oryzalin-treated seedlings. Control seedlings were germinated on media containing 0.017% methanol and grown for 5 d. Oryzalin seedlings were germinated on 175 nM oryzalin and grown for 5 d. Transferred seedlings were germinated on 0.017% methanol and transferred to plates containing 175 nM oryzalin for another 3 d. Error bars indicate SE.

of the array increased along the developmental axis. These older elongating cells maintained transverse arrays although cells often had arrays with slightly oblique orientations (Fig. 4D). The observed organization patterns closely resemble previous descriptions of fixed and stained Arabidopsis roots (Sugimoto et al., 2000) indicating that the GFP:MAP4 marker was suitable for imaging root cortical microtubule arrays.

To assess whether low oryzalin concentrations affect microtubule organization in wild-type tissue, we germinated and grew seedlings for 5 d on media containing 150 nM oryzalin and analyzed the microtubules in elongating root cells. The treatment did not result in any detectable alterations of microtubule behavior in the GFP:MAP4 control line (Fig. 4, A and D). By contrast, the 16-2 mutant seedlings exhibited disordered and longitudinally oriented cortical microtubules even in the absence of oryzalin (Fig. 4B), mainly associated with cells in the middle to late elongation zone. Exposure of 16-2 mutant seedlings to low oryzalin concentrations (150 nM) resulted in more severe root swelling, and extended disruption of parallel microtubule organization to the rapidly growing cells in the early elongation zone (Fig. 4C). Microtubule organization in untreated 52-isx mutant seedlings appeared similar to the GFP:MAP4 control line (compare Fig. 4, D and E). However, the terminal lengths of the root epidermal cells were shorter compared to control seedlings, consistent with the short root and hypocotyl phenotype of this mutant (Desnos et al., 1996; Fagard et al., 2000). Germination of 52-isx seedlings on 150 nM oryzalin resulted in compression of the elongation zone, loss of parallel order, and a premature switch from transverse to longitudinal cortical array orientation (compare Fig. 4, E and F; Table I).

In contrast to seedlings germinated on oryzalin-containing media where disorganization was most often observed near the end of the elongation zone, plants grown for 5 d on control media and then exposed to 175 nM oryzalin for 3 to 4 h were found to have cortical arrays lacking parallel order throughout the root elongation zone. To minimize any effect handling may have had on these seedlings, we germinated seedlings directly on coverglass with a thin coating of 0.5× Murashige and Skoog (MS) agarose to serve as a support and avoid any need to directly handle the seedlings. After 4.5 h of 175 nM oryzalin, the cortical arrays lost parallel order throughout the elongation zone in the 52-isx seedling roots (Fig. 5). Similar treatment of GFP:MAP4 control seedlings did not noticeably affect the parallel order of the cortical arrays. This observation is consistent with the cell swelling response that occurs when seedlings are transferred from control media to media with oryzalin as in our original screen. We observed that most mutant lines from our screen exhibited more severe swelling when transferred to oryzalin as compared with being germi-

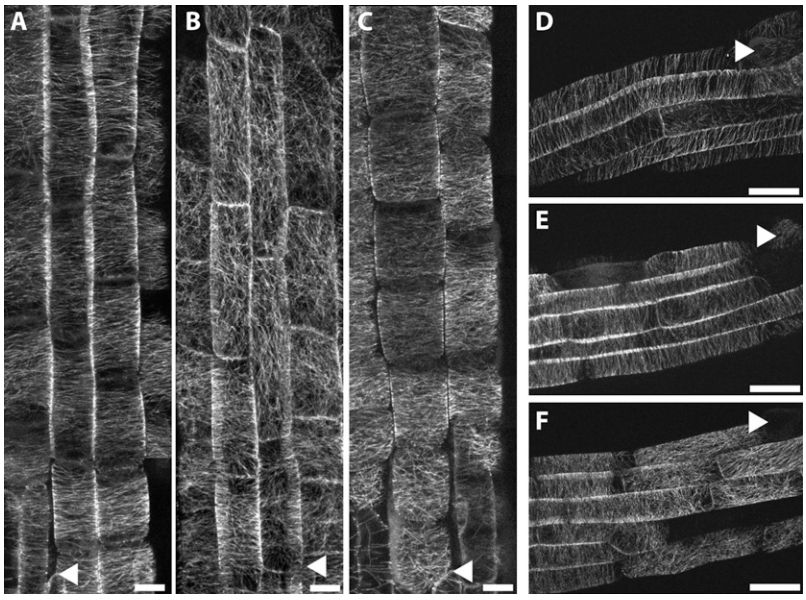

Figure 4. Effect of oryzalin on microtubule organization in the 16-2 and 52-isx mutants visualized by confocal microscopy of GFP:MAP4. Five-day-old Col-0 (A and D), 16-2 (B and C), and 52-isx (E and F) seedlings were grown under 24-h light on vertical plates containing the indicated inhibitors. Cortical microtubules of the GFP:MAP4 marker line (A and D) were unaffected by 150 nM oryzalin. The 16-2 mutant exhibits disorganized cortical microtubules in the absence of oryzalin (B), and treatment with 150 nM oryzalin causes lateral expansion of elongating root cells (C). E, Microtubule array organization appears normal in 52-isx without oryzalin treatment. F, Treatment with 150 nM oryzalin results in microtubule array reorganization from transverse to longitudinal near the end of the root elongating zone in the 52-isx mutant. Arrowheads mark the end of the root cap and the beginning of the elongation zone (A to C) and root hair emergence marking the end of the elongation zone (D to E). Scale bar = 10 μm.

Table I. *Microtubule orientation at the last position of the root expansion zone*

Line (n = no. of roots)	Transverse[a]	Oblique[b]	Disordered[c]	Longitudinal[d]
MAP4 control (n = 24)	74 (65.5%)	8 (7.1%)	31 (27.4%)	0
52-isx (n = 26)	25 (22.3%)	2 (1.8%)	71 (63.4%)	14 (12.5%)

[a]Microtubules in parallel arrays and oriented near 90° to the long axis of the cell. [b]Microtubules in parallel arrays with angles near 45°. [c]Microtubules not in parallel arrays; no dominant orientation could be determined. [d]Microtubules in parallel arrays and oriented with the long axis of the cell.

nated and grown in the presence of the drug (Figs. 1, G–I, and 2E), indicating that root cells have some ability to adapt to the destabilizing effects of oryzalin.

As a further test of sensitivity to agents that destabilize cortical microtubule organization, we treated 52-isx with 1-butanol, a compound initially thought to activate phospholipase-D, a protein shown to bind both microtubules and the plasma membrane (Dhonukshe et al., 2003; Gardiner et al., 2003). More recently 1-butanol has been demonstrated to act as a general inhibitor of microtubule polymerization (Hirase et al., 2006). In either case, the effect of 1-butanol is to cause microtubules to become detached from the plasma membrane when the GFP:MAP4 protein is also expressed in the same cells (Dhonukshe et al., 2003; Gardiner et al., 2003; Hirase et al., 2006; see DeBolt et al. [2007] for a similar GFP:MAP4-dependent result following exposure with the coumarin morlin). Though interpreting hypersensitivity to 1-butanol is complicated, treatment of 52-isx with 0.2% 1-butanol resulted in 85% (n = 40) of cortical arrays loosing parallel order while only 16.3% (n = 49) of the GFP:MAP4 control cells became disorganized (Fig. 6). Taken together with the sensitivity to oryzalin, these observations serve as additional evidence that 52-isx has a compromised cortical microtubule cytoskeleton.

Positional Cloning of Gene Conferring Mutant Phenotypes in 16-2 and 52-isx

To identify the recessive mutations responsible for the phenotypes of lines 16-2 and 52-isx, we employed a map-based cloning strategy. The mutation in 16-2 was mapped to a region between marker K6M13-3 and K2I5-1, a region on chromosome five containing 24 genes. The 16-2 mutation was identified, by sequencing the genes within the region, as a missense mutation converting Thr-343 to Ile in the *KORRIGAN* (*KOR*) gene (Nicol et al., 1998). Interestingly, *KOR* encodes an endo-1,4-β-D-glucanase, which is required for cellulose production via an unknown mechanism. Complementation tests with the *kor1-1* allele verified that line 16-2 carries a mutant allele of *kor* that we have designated *kor1-3* (Supplemental Fig. S2).

A similar map-base cloning strategy was employed to identify the mutation in line 52-isx. Initial mapping with a small population of 100 plants placed the mutation in a 10-centimorgan (cM) region between MJH22 at 119 cM and K1F13 at 129 cM. A marker was generated on BAC MUB3 (MUB3-F tgcatagttgaatagttcgtgaaaa, MUB3-R atgggcagatggagattgag) to split the interval and no recombinants were found with this marker indicating tight linkage to this region. Another known mutant, *procuste1-1* (*prc1-1*) with short dark-grown hypocotyls and isoxaben sensitivity had previously been mapped to the neighboring BAC MVP7. F_1 hybrids from crosses between *prc1-1* and 52-isx failed to show complementation. A splice site mutation was identified by sequencing the *prc1* gene in line 52-isx. The Arabidopsis consensus splice boundaries are a GT or GC donor site and an AG acceptor site (Hebsgaard et al., 1996). The seventh intron sequence for *PRC1* is cagGT…INTRON…AGgtc. Line 52-isx has a G to A mutation at the end of the third intron creating a 1-bp shift of the splice site acceptor so that the sequence becomes cagGT…INTRON…AAGtc. In turn there is a

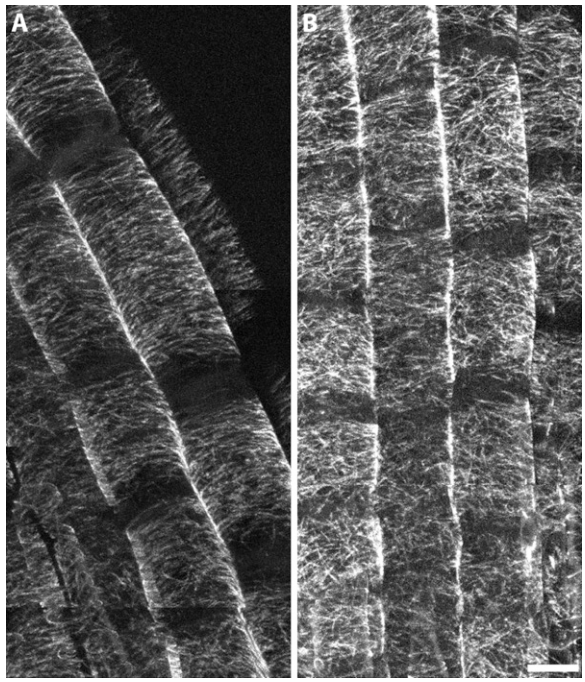

Figure 5. Abrupt oryzalin exposure causes randomized cortical microtubule organization in the 52-isx mutant. GFP:MAP4 control and 52-isx seedlings were grown on vertical plates with 24-h light directly on coverglass within a thin film of growth medium. Five-day-old seedlings were treated with 175 nM oryzalin for 4.5 h and then imaged by confocal microscopy. Cortical microtubules in the GFP:MAP4 (A) control line remain transverse after oryzalin exposure. Similar treatment of 52-isx mutant seedlings (B) resulted in randomized microtubules throughout the root elongation zone. Scale bar = 10 μm.

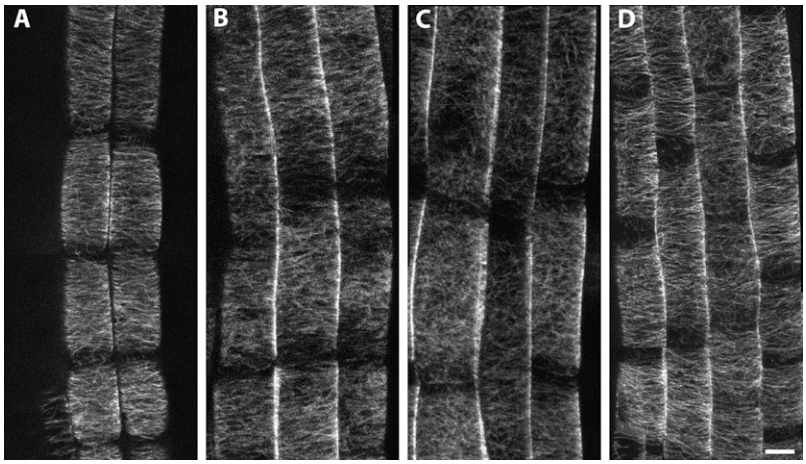

Figure 6. Cortical microtubules of 52-isx are sensitive to 1-butanol. A, Five-day-old GFP-MAP4 untreated. B and C, Five-day-old seedlings carrying GFP:MAP4 were transferred to media containing 0.2% 1-butanol for 22 to 24 h. Some loss of order occurs in MAP4 control (B) but 52-isx (C) is further disorganized by the same treatment, suggesting less stable cortical arrays. (D) Treatment of 52-isx with 0.2% 2-butanol does not affect MT organization demonstrating the specificity of the 1-butanol affects. Scale bar = 10 μm.

1-bp deletion in the transcript leading to a series of missense mutations starting at amino acid 503 and eventually ending with an early stop at amino acid 522.

PRC1 encodes CESA6, which, similar to KOR, is necessary for cellulose biosynthesis. Like the previously reported *prc1* mutants, the 52-isx allele results in short radially swollen dark-grown hypocotyls (Fig. 2A), and appears indistinguishable from the original *prc1* null mutant, *prc1-1* (Fagard et al., 2000). The causal role of the 52-isx mutation was confirmed both by complementation tests with *prc1-1* (Supplemental Fig. S3) and by complementation with a YFP:CESA6 construct (data not shown; Paredez et al., 2006). We designated the *prc1* allele in 52-isx as *prc1-20*.

Pharmacological Inhibition of CESA Causes Changes in Cortical Microtubule Array Organization in the Arabidopsis Root Elongation Zone

The herbicide isoxaben specifically inhibits cellulose synthesis, likely by direct interaction with CESA3 and CESA6 (Scheible et al., 2001). In addition, isoxaben treatment results in a rapid depletion of plasma membrane localized CESA complexes (Paredez et al., 2006). Fisher and Cyr (1998) reported randomization of microtubules in tobacco (*Nicotiana tabacum*) cells after 2 h of 2.5 μM isoxaben treatment and 2,6-dichlorobenzonitrile (DCB) treatment caused alteration of microtubule orientation in Arabidopsis roots (Himmelspach et al., 2003). To investigate whether isoxaben also affects microtubule organization in Arabidopsis roots, and to compare this pharmacological disruption to disruption by our genetic mutations, we treated Arabidopsis seedlings with 100 nM isoxaben. After 1.5 h of treatment, cells near the top of the root elongation zone exhibited reorienting microtubule arrays, and by 2.5 h, cells in the early elongation zone had switched from transverse to oblique or longitudinal arrays (compare Fig. 7, A and B). By contrast, the control treatment did not result in reorientation of the microtubule arrays (Fig. 7A). These results differ somewhat from those observed by Fisher and Cyr (1998) in tobacco tissue culture cells, where 2 h of 2.5 μM isoxaben treatment caused randomization of the cortical array rather than reorientation, and those of Himmelspach et al. (2003) who observed greater dispersion of orientation angles following DCB treatment.

Partial Cellulase Digestion Does Not Cause Cortical Array Disorganization

The identification of KOR and PRC1 as gene products involved in microtubule orientation indicates that cellulose synthesis influences microtubule cortical array organization either directly or indirectly. To ask if the effects on microtubule orientation were caused indirectly by a general stress response resulting from loss of cell wall function, we examined root microtubules after hydrolysis of cellulose microfibrils by cellulase. If loss of cell wall integrity causes a stress response that results in alteration of skeletal organization, then cells that show incipient swelling as a result of cellulase treatment ought to show such a stress response. To test if cellulase treatment generates reorganization of microtubules we applied 0.1% cellulase R10 to Arabidopsis seedlings. Addition of the cellulase resulted in an 11.7% ($n = 28$ control; $n = 34$ cellulase treated) increase in cell width compared with mature cells of the same cell file. In contrast, the cells at this same position in untreated roots were 3.9% thinner, which is in agreement with the negative tangential expansion of this region reported by Baskin et al. (2004). Therefore, the actual amount of swelling induced by the cellulase treatment was around 15% assuming that the more mature cells were resistant to the cellulase ($P < 0.001$ by equal variance t test comparing the ratios of cellulase-treated cell widths to untreated controls). Root widths of *prc1-20* in the absence of inhibitors were measured to be 14.8% wider than the wild type suggesting that the cellulase treatment compromised the cell wall integrity similarly to the *prc1-20* mutant. Despite significant cell swelling, reorganization of microtubule arrays did not occur (Fig. 7C), suggesting that neither decreased cellulose integrity in the wall, nor the cell swelling per se are sufficient to cause microtubule reorientation. To assess whether the cellulase treatment resulted in increased sensitivity

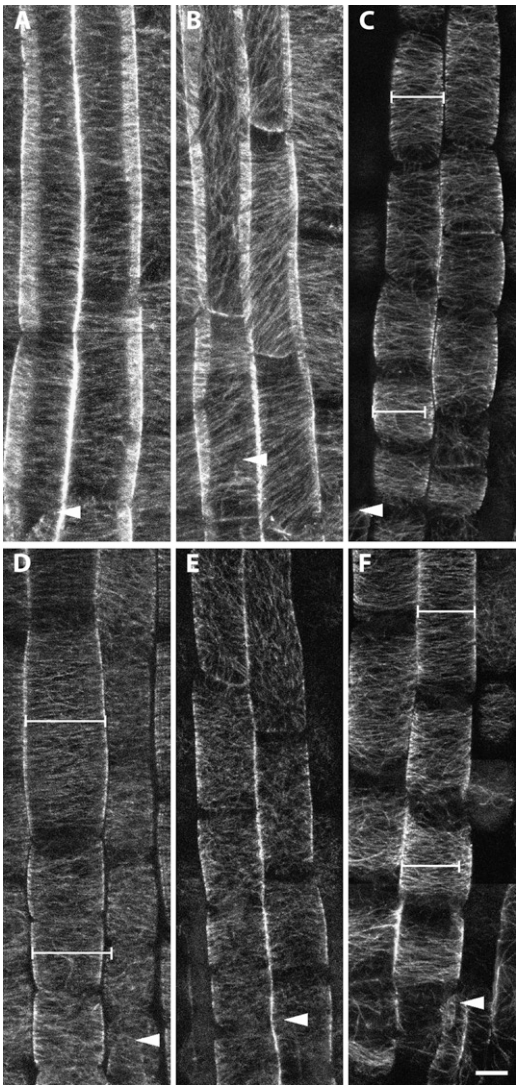

Figure 7. Disruption of CESA activity affects microtubule organization. All seedlings were grown on 0.5× MS under 24-h light for 5 d and carried GFP:MAP4 to facilitate visualization of microtubules. A, Control seedlings mounted in 0.01% dimethyl sulfoxide for 2.5 h. B, MAP4-GFP seedlings mounted in 100 nM isoxaben for 2.5 h, resulting in oblique and longitudinally organized microtubules. C, MAP4-GFP seedlings treated with .1% cellulase R10. D, MAP4-GFP seedlings treated with 150 nM oryzalin for 3.5 h. E, Five-day-old *prc1-20* seedlings mounted in 150 nM oryzalin for 3.5 h. The oryzalin treatment results in randomized microtubules. F, Five-day-old control seedlings treated with 0.1% cellulase R10 and 150 nM oryzalin. Caliper bars are set to the width of the cell at the top of the file. Scale bar = 10 μm.

to destabilizing agents we exposed the seedlings to 150 nM oryzalin (Fig. 7F). The cellulase-treated cells were also able to maintain transverse microtubule arrays after oryzalin exposure. By contrast, the same oryzalin exposure without cellulase treatment randomized the cortical arrays throughout the elongation zone in *prc1-20* (Fig. 7E).

It should be noted that roots are fairly fragile and cellulase R10 is routinely used for protoplasting cells, hence the treated roots are more fragile. When higher concentrations of cellulase were applied for longer time periods, whole cell files would begin to slough off and eventually the root tips would fall apart. Indeed, mishandling of even untreated reporter line seedlings resulted in abnormal microtubule patterns, and extreme care was therefore taken to minimize manipulation of the material used for the experiments. We did not perform the cellulase experiments on agarose-encased seedlings as in Figure 5 because the cellulase and oryzalin are expected to diffuse through the medium at different rates. With these caveats taken into consideration, the results suggest that a reduction in cellulose content is not sufficient to cause microtubule disorganization while oryzalin treatment of *prc1-20* causes disorganization throughout the elongation zone. These data suggest that microtubule array orientation and organization responded to the presence or activity of CESA6, and not to cellulose content or cell wall integrity.

Mutations in *KOR* Affect CESA Activity

The common link between KOR and PRC1 is their role in cellulose production. If the orientation and stability of microtubules is dependent on the presence and activity of plasma membrane-associated CESA complexes, we would expect to see changes in CESA activity or behavior, for *kor1-3*. To directly monitor the dynamics of the CESA complex in the *kor1-3* background, we made reciprocal crosses between *kor1-3* and a YFP:CESA6 marker line (Paredez et al., 2006). Plasma membrane-associated CESA complexes migrated with an average velocity of 353 ± 79 nm/min (n = 242) in the control line (Fig. 8C). These measurements were obtained by kymograph analysis of 10-min data sets from dark-grown hypocotyls. Similar analyses in the *kor1-3* revealed significantly reduced CESA complex velocities (Fig. 8C), with an average velocity of 280 ± 87 nm/min (n = 227; $P < 0.001$ by equal variance t test compared to control; Fig. 7F). In addition, kymograph analyses showed that individual complexes exhibited aberrant behaviors in *kor1-3*. Whereas CESA complexes typically migrate with constant speed, resulting in parallel particle streaks (Fig. 8D), the traces of complexes in the *kor1-3* sometimes showed arcing lines with a gradually diminishing slope (n = 6 of 227; Fig. 8F). This suggests that some CESA complexes exhibited a loss of velocity during cellulose deposition. In addition, some complexes were observed to have slow velocities and only move relatively short distances (bright spots observed in time-averaged images of YFP:CESA6 such as the red circle in Fig. 8B and the associated kymograph in Fig. 8E). Indeed, only one of 243 wild-type particles was observed to have a velocity below 150 nm/min while 15 of 228 *kor1-3* particles were observed at or below 150 nm/min. Because the maximal velocities measured in both populations of complexes was approximately the same (about 500 nm/min), and instances of complexes slow-

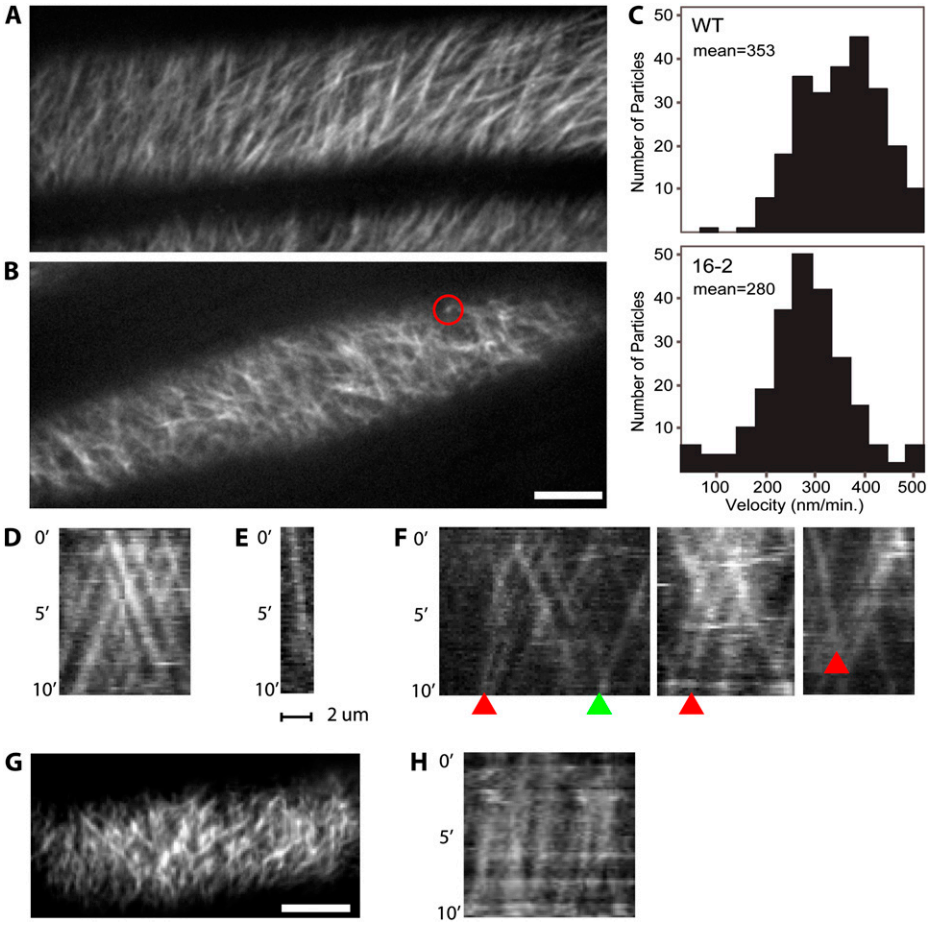

Figure 8. CESA6:YFP dynamics are altered in *kor1-3* and *kor1-1*. A and B, Average of 60 frames acquired over 10 min in wild type (A) and *kor1-3* (B). Red circle in B marks a slow moving particle (78 nm/min) that is seen as a bright spot in the average projection. Scale bar = 10 μm. C, Histogram of measured particle velocities; the mean is 353 nm/min in wild type and 280 nm/min in *kor1-3*. D to F, Kymographs from 10-min observations of wild type (D) and *kor1-3* (E and F). Particle velocities are constant in the wild type (D); note the linear streaks. Kymograph (E) corresponds to the slow moving particle marked by the red circle in B; note the shallow slope indicating slow movement. Particle velocities can be seen to slow down in *kor1-3* during the period of imaging (F; arcing streaks indicated by red arrowheads), while the particle marked with a green arrowhead remained at a constant velocity. G, Average projected image of *kor1-1* as in A and B. H, Kymograph of YFP:CESA6 in *kor1-1* showing consistently slow velocities measured to be 143 ± 43 nm/min (n = 50). Scale bar = 10 μm.

ing over time were documented, it is possible that KOR plays a role in maintaining optimal CESA function.

Reciprocal crosses between the original *kor1-1* mutant, which has a more severe hypocotyl growth defect, (Supplemental Fig. S2; Nicol et al., 1998) and YFP:CESA6 resulted in even more apparent effects on CESA organization and velocity (Fig. 8, G and H). The mean velocity of YFP:CESA6 in *kor1-1* was measured to be 143 ± 43 nm/min (n = 50), corroborating the reduced velocities and aberrant behavior of CESA complexes observed in the *kor1-3* background.

To test if there was a corresponding loss of cellulose production in *kor1-3*, we measured the cellulose content of *kor1-3* in 6-d-old etiolated seedlings. The *kor1-3* seedlings did not show any significant reduction in cellulose content when compared to the wild type, but did exhibit alterations in the Fourier transform infrared (FTIR) spectrum. Principal component analysis revealed that 88% of the variance corresponded to cellulosic signals at 1033, 1060, and 1162 cm^{-1} (data not shown). As expected, cellulose content analysis of *prc1-20* found significantly decreased cellulose content (64% ± 11%) compared to wild-type control seedlings. Unfortunately, both YFP:CESA6 and YFP-CESA2 markers available to us rescue the *prc1* phenotype, so we were unable to monitor changes in CESA complex velocities for the *prc1-20* background.

DISCUSSION

Here we show that two mutants, which are hypersensitive to the microtubule destabilizing drug oryzalin, have defects in their microtubule cytoskeleton. The mutants are part of a larger mutant collection (131 in total) that exhibit microtubule organization defects, but remain uncharacterized. A similar hypersensitive screen was performed by Stearns et al. (1990) in yeast (*Saccharomyces cerevisiae*) using benomyl, which identified three tubulin folding genes (*CIN1*, *CIN2*, and *CIN4*) and all three of the yeast tubulin genes (Tian et al., 1996; Fleming et al., 2000). More recently, Naoi and Hashimoto (2004) screened Arabidopsis with the microtubule-targeted herbicide propizamide, which functions through an unknown mechanism, and identified *PROPYZAMIDE-HYPERSENSITIVE1* as a MAP-kinase-like gene involved in cortical microtubule organization. The identification of 16-2 (*kor1-3*) and 52-isx (*prc1-20*) as factors affecting the organization of microtubules in the root elongation zone demonstrates the utility of hypersensitive mutant screens.

Because both *prc1* and *kor* were previously shown to have a role in cellulose biosynthesis, we were initially surprised to learn that these mutants were also found in our screen for regulators of the cortical microtubule cytoskeleton. There are no previous reports of altered

microtubule organization in *prc1* and *kor* mutants. The cortical arrays of *prc1-20* are typical of the wild type, and a defect only becomes apparent after treatment with microtubule inhibitors. We did not specifically examine the microtubule arrays of other *prc* alleles, but all 20 reported alleles have early stop codons and are thought to be null mutants (Fagard et al., 2000). Furthermore, the original mutant *prc1-1* has an identical root swelling phenotype when exposed to oryzalin (Supplemental Fig. S3).

The cortical microtubule phenotype of *kor* is more complex due to the varying lesion types and their associated phenotypes. For example, *kor1-1* has a more severe short hypocotyl phenotype but the roots are not oryzalin hypersensitive and the root cortical arrays are similar to the wild type (Bichet et al., 2001). In contrast, the *radially swollen2* (*rsw2*) allele was identified based on temperature-sensitive root swelling and, interestingly, the mutation responsible for the cold sensitivity of *kor1-3* is directly adjacent to the mutation that confers temperature sensitivity in *rsw2*. Unfortunately there are no published images of *rsw2* cortical arrays. However, another allele *lion's tail1* (*lit1*) was identified as Suc sensitive and it displays root swelling when grown on Suc-containing media (Hauser et al., 1995). An image of *lit1* root cortical arrays is published and while the authors reported that the microtubules kept parallel order, the cortical arrays look less robust and less organized when compared with the wild type or any of the other four Suc-sensitive mutants depicted.

The influence of cortical microtubules on the organization of CESA has clearly been demonstrated by live cell imaging studies (Paredez et al., 2006; DeBolt et al., 2007). The possibility that cellulose may influence the orientation of microtubules was hypothesized by Emons et al. (1992). The first evidence for a bidirectional flow of information between microtubules and microfibrils (or CESA) was reported by Fisher and Cyr (1998), who observed that the cortical microtubule arrays of tobacco protoplasts could not acquire parallel order while in the presence of the CESA inhibitor isoxaben, leading the authors to propose a biophysical model for feedback into microtubule orientation. The observation that DCB, an inhibitor of cellulose biosynthesis, caused altered microtubule orientation in Arabidopsis roots is also evidence that cellulose synthesis influences microtubule orientation (Himmelspach et al., 2003). More recently, Chu et al. (2007) observed that a null mutation of *CESA2* exhibited altered microtubule organization and concluded that there is a connection between cellulose and microtubule organization. However, the authors did not propose a mechanism to explain this phenomenon.

Recently several CESA6-related CESAs (CESA2, CESA5, and CESA9) were inferred as functionally redundant (Desprez et al., 2007; Persson et al., 2007). Yet, the functional overlap between the CESAs was only partial, which may indicate specific characteristics for CESA6, possibly through interactions with other proteins such as the microtubules or MAPs. Indeed, *rsw1-1*, which encodes CESA1, has been shown to display normal cortical microtubule organization (Arioli et al., 1998; Sugimoto et al., 2001). However, the microtubule phenotype of *prc1-20* only becomes apparent after exposure to oryzalin, and care must be taken before drawing conclusions from *rsw1-1* because it is not a null mutant; Sugimoto et al. (2001) only reported on the middle portion of the elongation zone where even oryzalin-treated *prc1* cells can appear normal. We did not examine microtubule organization or YFP:CESA6 dynamics in *rsw1-1* due to the lack of a temperature-controlled stage. Future studies of CESA dynamics in the *rsw1-1* background should prove insightful.

Several mechanisms for the influence of cellulose synthesis on cytoskeletal organization are plausible. These include the biophysical model proposed by Fisher and Cyr (1998), involvement of receptor signaling pathways, or direct interactions between the microtubules and the CESA complex. The original study performed by Fisher and Cyr relied upon a combination of cell wall degradation and chemical inhibition of CESA with isoxaben. Although it was understood that isoxaben treatment blocked cellulose deposition, it had not yet been shown that CESA3 and CESA6 are the targets of isoxaben (Desprez et al., 2002; Scheible et al., 2001), and more importantly that treatment with isoxaben depletes CESA6-containing complexes from the plasma membrane (Paredez et al., 2006). Fisher and Cyr (1998) reported that microtubules only became oriented after a protoplasted cell had established a major strain axis, and that isoxaben treatment only disorganized microtubules after isodiametric swelling began. The properties of the *prc1-20* mutant serve as evidence arguing against the biophysical strain model. Cells in the root elongation zone of *prc1-20* are clearly able to establish a major strain axis in the middle to upper elongation zone, and while the microtubules of untreated roots appear indistinguishable from the wild type, abrupt oryzalin exposure results in disorganization of the cortical arrays throughout the root elongation zone of *prc1-20* (Figs. 5B and 7E). Moreover, we can approximate the degree of cell swelling observed in *prc1-20* roots through cellulose degradation, and the cortical arrays remain transverse despite exposure to oryzalin (Fig. 7, C and F). Depletion of plasma membrane-localized CESA (*prc1-20* or isoxaben) or modification of CESA dynamics (*kor1-3*) results in altered microtubule organization and sensitivity to oryzalin.

It remains possible that a defect in cellulose production or the stress that results from compromised cell walls is sensed and may trigger a cascade of intracellular events, resulting in destabilization of the microtubules. Recently, a lesion in the receptor-like kinase *THESEUS* (*THE*) was identified that suppresses the *prc1-1* short hypocotyl phenotype, confirming the presence of cell wall sensors (Hematy et al., 2007). Suppressed *prc1-1 the1-1* (or *the1-2*) plants retain sensitivity to oryzalin (data not shown). However, it is possible that other similar receptors may act in the root

to detect deficiencies in cell wall production or growth and communicate this to other structural components, such as the microtubules.

The strong correlation between the cortical arrays and the orientation of CESA complex movement suggest a third class of mechanism based upon direct interaction (Paredez et al., 2006; Paradez et al., 2006). Because microtubules can act as guides for CESA complexes, it is expected that microtubules would have at a minimum transient interactions with CESA complexes. This interaction would provide the opportunity for stabilizing microtubule interactions at the cell cortex. An absence or alteration of CESA could therefore change the spectrum or quality of interacting partners at the cell cortex, and thus the relative stability and capacity of the array to achieve a particular organizational state or to respond to signals that change array organization. Experiments with two recently discovered drugs, morlin and cobtorin, also support the idea of direct interaction between microtubules and CESA (De Bolt et al., 2007; Yoneda et al., 2007), as does the observation that isoxoben apparently depletes biosynthetic complexes from the cell membrane (Paredez, 2006) Finally, the relative insensitivity of microtubule orientation to partial cellulase digestion suggests that cellulose content and the cell wall integrity are of less influence on microtubule orientation than are genetic and pharmacological depletion of the CESA6 protein from the cell membrane.

Though microtubule-plasma membrane attachments have been observed regularly in EM images (Hardham and Gunning, 1978; Marchant, 1978) the total number of proteins that may participate in microtubule attachment to the plasma membrane is unknown. To date the only protein shown to interact with both microtubules and the plasma membrane is a 90-kD phospholipase-D protein, which has an unknown in vivo contribution to the microtubule-plasma membrane attachment (Gardiner et al., 2001). It is tempting to speculate that CESA complexes in general and possibly CESA6 in particular acts as part of a system that participates in the stabilization of microtubules at the surface of the plasma membrane. Indeed the oryzalin hypersensitivity of *prc1-20* and *kor1-3* is suggestive of less stable microtubule arrays. This interpretation is supported by the study of MAP18, which has been demonstrated to inhibit microtubule polymerization in vitro (Wang et al., 2007). The microtubule phenotype of MAP18 overexpression (destabilized microtubules) results in root cortical arrays with longitudinally organized microtubules such as those seen in Figure 4, B and F. Furthermore, MAP18 overexpression lines were found to be hypersensitive to oryzalin while the RNAi knockdowns were resistant. Because oryzalin sensitivity appears to be correlated with array stability, it reasonably follows that both *prc1-20* and *kor1-3* have less stable cortical microtubule arrays.

The results presented here substantiate previous reports that the state of the cell wall and/or cell wall biosynthesis influences microtubule organization and present evidence that CESA is part of this influence. Hopefully the new tools for live cell imaging of both CESA and microtubules, along with the rapidly expanding collection of mutants and bioactive chemicals will facilitate further insights into the underlying mechanisms. While cellulose production, microtubule bundling, and intermicrotubule interactions all appear to have some input into microtubule organization the mechanisms that specify cortical microtubule orientation remain an enduring mystery.

MATERIALS AND METHODS

Mutant Screening

EMS mutagenized and surface sterilized seeds were imbibed at 4°C for 3 d. Seeds were sown on strips of sterilized Whatman paper on 0.5× MS plates. Seedlings were grown for 4 d at 22°C and 24-h light before being transferred en masse via the paper strips to 0.5× MS and 175 nM oryzalin plates for an additional 2 to 3 d. Seedlings with short and swollen roots were rescued to 0.5× MS and allowed to recover before transplanting to soil. Rescreening was performed by germinating M1 progeny on both the MS and oryzalin media and comparing growth. Isoxaben screening was performed the same way by substituting 2 nM isoxaben plates. Oryzalin was prepared in methanol and isoxaben in dimethyl sulfoxide.

Microscopy

Microtubule imaging was performed on a Nikon Diaphot 200 fluorescence microscope equipped with a 60× 1.2 numerical aperture water objective and a Bio-Rad MRC 1024 confocal head. Immunofluorescence images were prepared as in Sugimoto et al. (2001). Z stacks were processed into maximum projections with ImageJ (Rasband, 1997–2007) except for Figure 6, B to D. The images in Figure 6, B to D, were processed as SD projections. Mosaic images were assembled in Photoshop (Adobe Systems). YFP:CESA6 particle dynamics were imaged on a spinning disc confocal microscope and measured as described in Paredez et al. (2006). Seedling images were acquired on a Leica dissecting microscope equipped with a Leica DC500 digital camera (Leica Microsystems).

Fine Mapping and Gene Identification

For 52-isx mapping, an initial mapping population of 96 plants identified an interval containing four recombinants to the right of MJH22 (119 cM; MJH22-F aaggcaagcttgtgcctcta, MJH22-R caacgggaatgatctttcttt) and seven recombinants to the left of KIF13 (129 cM; K1F13-F aatggagacttttgcgagga, K1F13-R ccaaaagccaccagaaattg). An additional marker was generated on BAC MUB3 (MUB3-F tgcatagttgaatagttcgtgaaaa, MUB3-R atgggcagatggagattgag) and zero recombinants were found indicating tight linkage to this region. MVP7, the neighboring BAC, contained *prc1*, a locus defined by short dark-grown hypocotyls and isoxaben hypersensitivity. Sequencing of 52-isx identified a splice site mutation in the third intron of *PRC1*.

For 16-2 mapping of a population containing 1,824 oryzalin-hypersensitive individuals, two recombinants were identified to the right of K6M13-3 (K6M13-3F gaagatcatccgatggcact, K6M13-3R gcgtcgattgcttatttcgt cut with *Cfr*I) and one recombinant was identified to the left of marker K2I5-2 (K2I5-2F tagatgctctttccgcacgact, K2I5-R tttagaatttccagacctgatgc cut with *Hin*fI). This region includes 24 genes AT5G4930 to AT5G4975. Sequencing identified a polar to hydrophobic substitution in KOR (Thr-343 to Ile).

Cellulase and Drug Treatments

Short-term (3–5 h) treatments were performed in six-well tissue culture plates using water and a specified drug or enzymatic treatment except in Figure 4. The seedlings in Figure 4 were grown on coverglass coated with 0.5× MS agar and placed upon a standard 0.5× MS plate to maintain humidity. The coverslips were dipped into conical tubes containing 175 nM oryzalin for 4.5 h.

Cellulose Measurements

Cellulose contents were measured on ball-milled material from 6-d-old etiolated seedlings according to Updegraff (1969).

FTIR Spectroscopy

Six-day-old etiolated seedlings were extracted with 1:1 chloroform methanol overnight and then with acetone. After air drying at room temperature overnight, the material was ground to a fine powder with a ball mill for 1 to 2 h. Prior to collection of FTIR spectra the powder was mixed with potassium bromide and pressed into 13-mm pellets. Fifteen spectra for each line were collected on a Thermo-Nicolet Nexus 470 spectrometer over the range 4,000 to 400 cm^{-1}. For each spectrum, 32 scans were co-added at a resolution of 8 cm^{-1} for Fourier transform processing and absorbance spectrum calculation using Omnic software (Thermo Nicolet). Spectra were corrected for background by automatic subtraction and saved in JCAMP.DX format for further analysis. Using Win-Das software (John Wiley & Sons), spectra were baseline corrected, area normalized, and analyzed using the principal components analysis covariance matrix method (Kemsley, 1998).

Supplemental Data

The following materials are available in the online version of this article.

Supplemental Figure S1. Mutant 16-2 is rescued by growth at high temperature.

Supplemental Figure S2. Mutant 16-2 carries an allele of *kor*.

Supplemental Figure S3. Mutant 52-isx carries an allele of *prc1*.

ACKNOWLEDGMENTS

We thank J. Milne for assistance with FTIR, and S. Cutler, D. Bonetta, M. Nishimura, M. Facette, K. Hematy, R. Gutierrez, and J. Gendron for stimulating conversation and advice.

Received April 2, 2008; accepted June 22, 2008; published June 26, 2008.

LITERATURE CITED

Arioli T, Peng L, Betzner A, Burn J, Wittke W, Herth W, Camilleri C, Höfte H, Plazinski J, Birch R, et al. (1998) Molecular analysis of cellulose biosynthesis in Arabidopsis. Science **279:** 717–720

Bao Y, Kost B, Chua NH (2001) Reduced expression of α-tubulin genes in *Arabidopsis thaliana* specifically affects root growth and morphology, root hair development and root gravitropism. Plant J **28:** 145–157

Baskin TI (2001) On the alignment of cellulose microfibrils by cortical microtubules: a review and a model. Protoplasma **215:** 150–171

Baskin TI, Beemster GTS, Judy-March JE, Marga F (2004) Disorganization of cortical microtubules stimulates tangential expansion and reduces the uniformity of cellulose microfibril alignment among cells in the root of *Arabidopsis thaliana.* Plant Physiol **135:** 2279–2290

Baskin TI, Wilson JE, Cork A, Williamson RE (1994) Morphology and microtubule organization in Arabidopsis roots exposed to oryzalin or taxol. Plant Cell Physiol **35:** 935–942

Bichet A, Desnos T, Turner S, Grandjean O, Hofte H (2001) BOTERO1 is required for normal orientation of cortical microtubules and anisotropic cell expansion in Arabidopsis. Plant Journal **126:** 278–288

Burk DH, Liu B, Zhong RQ, Morrison WH, Ye ZH (2001) A katanin-like protein regulates normal cell wall biosynthesis and cell elongation. Plant Cell **13:** 807–827

Chan J, Calder G, Fox S, Lloyd C (2007) Cortical microtubule arrays undergo rotary movements in Arabidopsis hypocotyl epidermal cells. Nat Cell Biol **2:** 171–5

Chu Z, Chen H, Zhang Y, Zhang Z, Zheng N, Yin B, Yan H, Zhu L, Zhao X, Yuan M, et al (2007) Knockout of the AtCESA2 gene affects microtubule orientation and causes abnormal cell expansion in Arabidopsis. Plant Physiol **143:** 213–224

DeBolt S, Gutierrez R, Ehrhardt DW, Melo CV, Ross L, Cutler SR, Somerville CR, Bonetta D (2007) Morlin, an inhibitor of cortical microtubule dynamics and cellulose synthase movement. Proc Natl Acad Sci USA **104:** 5854–5859

Desnos T, Orbovic V, Bellini C, Kronenberger J, Caboche M, Traas J, Höfte H (1996) *Procuste1* mutants identify two distinct genetic pathways controlling hypocotyl cell elongation, respectively in dark- and light-grown *Arabidopsis* seedlings. Development **122:** 683–693

Desprez T, Juraniec M, Crowell E, Jouy H, Pochylova Z, Parcy F, Höfte H, Gonneau M, Vernhettes S (2007) Organization of cellulose synthase complexes involved in primary cell wall synthesis in *Arabidopsis thaliana.* Proc Natl Acad Sci USA **104:** 15572–15577

Desprez T, Vernhettes S, Fagard M, Refrégier G, Desnos T, Aletti E, Py N, Pelletier S, Höfte H (2002) Resistance against herbicide isoxaben and cellulose deficiency caused by distinct mutations in same cellulose synthase isoform CESA6. Plant Physiol **128:** 482–90

Dhonukshe P, Laxalt AM, Goedhart J, Gadella TW, Munnik T (2003) Phospholipase D activation correlates with microtubule reorganization in living plant cells. Plant Cell **15:** 2666–2679

Dixit R, Cyr R (2004) Encounters between dynamic cortical microtubules promote ordering of the cortical array through angle-dependent modifications of microtubule behavior. Plant Cell **16:** 3274–3284

Dolan L, Duckett C, Grierson C, Linstead P, Schneider K, Lawson E, Dean C, Poethig S, Roberts K (1994) Clonal relationships and cell patterning in the root epidermis of Arabidopsis. Development **120:** 2465–2474

Ehrhardt DW (2008) Straighten up and fly right: microtubule dynamics and organization of non-centrosomal arrays in higher plants. Curr Opin Cell Biol **20:** 107–116

Emons AMC, Derksen J, Sassen MMA (1992) Do microtubules orient plant cell wall microfibrils? Physiol Plant **84:** 486–493

Fagard MT, Desnos T, Desprez T, Goubet F, Refregier G, Mouille G, McCann M, Rayon C, Vernhettes S, Höfte H (2000) PROCUSTE1 encodes a cellulose synthase required for normal cell elongation specifically in roots and dark-grown hypocotyls of *Arabidopsis.* Plant Cell **12:** 2409–2424

Fisher DD, Cyr RJ (1998) Extending the microtubule/microfibril paradigm. Cellulose synthesis is required for normal cortical microtubule alignment in elongating cells. Plant Physiol **116:** 1043–1051

Fleming JA, Vega LR, Solomon F (2000) Function of tubulin binding proteins in vivo. Genetics **156:** 69–80

Gardiner J, Collings DA, Harper JD, Marc J (2003) The effects of the phospholipase D-antagonist 1-butanol on seedling development and microtubule organization in Arabidopsis. Plant Cell Physiol **44:** 687–696

Gardiner JC, Harper JD, Weerakoon ND, Collings DA, Ritchie S, Gilroy S, Cyr RJ, Marc J (2001) A 90-kD phospholipase D from tobacco binds to microtubules and the plasma membrane. Plant Cell **13:** 2143–2158

Giaever G, Shoemaker DD, Jones TW, Liang H, Winzeler EA, Astromoff A, Davis RW (1999) Genomic profiling of drug sensitivities via induced haploinsufficiency. Nat Genet **21:** 278–283

Green PB (1962) Mechanism for plant cellular morphogenesis. Science **138:** 1404–1405

Green PB (1963) On mechanisms of elongation. *In* M. Locke, ed, Cytodifferentiation and Macromolecular Synthesis. Academic Press, New York, pp 203–234

Hardham AR, Gunning BE (1978) Structure of cortical microtubule arrays in plant cells. J Cell Biol **77:** 14–34

Hauser MT, Morikami A, Benfey PN (1995) Conditional root expansion mutants of Arabidopsis. Development **121:** 1237–1252

Hebsgaard SM, Korning PG, Tolstrup N, Engelbrecht J, Rouze P, Brunak S (1996) Splice site prediction in Arabidopsis thaliana pre-mRNA by combining local and global sequence information. Nucleic Acids Res **24:** 3439–3452

Hematy K, Sado PE, Van Tuinen A, Rochange S, Desnos T, Balzergue S, Pelletier S, Renou JP, Höfte H (2007) A receptor-like kinase mediates the response of Arabidopsis cells to the inhibition of cellulose synthesis. Curr Biol **17:** 922–931

Himmelspach R, Williamson RE, Wasteneys GO (2003) Cellulose microfibril alignment recovers from DCB-induced disruption despite microtubule disorganization. Plant J **36:** 565–575

Hirase A, Hamada T, Itoh TJ, Shimmen T, Sonobe S (2006) *n*-Butanol induces depolymerization of microtubules in vivo and in vitro. Plant Cell Physiol **47:** 1004–1009

Hugdahl JD, Morejohn LC (1993) Rapid and reversible high-affinity binding of the dinitroaniline herbicide oryzalin to tubulin from *Zea mays* L. Plant Physiol **102:** 725–740

Kemsley EK (1998) Discriminant Analysis and Class Modelling of Spectroscopic Data. John Wiley & Sons, New York

Le J, Vandenbussche F, De Cnodder T, Van Der Straeten D, Verbelen JP (2005) Cell elongation and microtubule behavior in the Arabidopsis

hypocotyl: responses to ethylene and auxin. J Plant Growth Regu **24:** 166–178

Ledbetter MC, Porter KR (1963) A ''microtubule'' in plant cell fine structure. J Cell Biol **19:** 239–250

Marc J, Granger CL, Brincat J, Fisher DD, Kao T, McCubbin AG, Cyr RJ (1998) A GFP-MAP4 reporter gene for visualizing cortical microtubule rearrangements in living epidermal cells. Plant Cell **10:** 1927–1940

Marchant HJ (1978) Microtubules associated with the plasma membrane isolated from protoplasts of the green alga Mougeotia. Exp Cell Res **115:** 25–30

Naoi K, Hashimoto T (2004) A semidominant mutation in an *Arabidopsis* mitogen-activated protein kinase phosphatase-like gene compromises cortical microtubule organization. Plant Cell **16:** 1841–1853

Nicol F, His I, Jauneau A, Vernhettes S, Canut H, Höfte H (1998) A plasma membrane-bound putative endo-1,4-β-D-glucanase is required for normal wall assembly and cell elongation in Arabidopsis. EMBO J **17:** 5563–5576

Paradez A, Wright A, Ehrhadt DW (2006) Microtubule cortical array organization and plant cell morphogenesis. Curr Opin Plant Biol **9:** 571–578

Paredez AR (2006) Genetic analysis and visual characterization of the relationship between the tubulin cytoskeleton and the plant cell wall. PhD thesis. Stanford University, Stanford, CA

Paredez AR, Somerville CR, Ehrhardt DW (2006) Visualization of cellulose synthase demonstrates functional association with microtubules. Science **312:** 1491–1495

Persson S, Paredez A, Carroll A, Palsdottir H, Doblin M, Poindexter P, Khitrov N, Auer M, Somerville C (2007) Genetic evidence for three unique components in primary cell wall cellulose synthase complexes in *Arabidopsis*. Proc Natl Acad Sci USA **104:** 15566–15571

Rasband WS (1997–2007) ImageJ. National Institutes of Health, Bethesda, MD. http://rsb.info.nih.gov/ij/

Scheible WR, Eshed R, Richmond T, Delmer D, Somerville C (2001) Modifications of cellulose synthase confer resistance to isoxaben and thiazolidinone herbicides in Arabidopsis *ixr1* mutants. Proc Natl Acad Sci USA **98:** 10079–10084

Shaw SL, Kamyar R, Ehrhardt DW (2003) Sustained microtubule treadmilling in Arabidopsis cortical arrays. Science **300:** 1715–1718

Shibaoka (1994) Plant hormone-induced changes in the orientation of cortical microtubules: alterations in the cross-linking between microtubules and the plasma membrane. Annu Rev Plant Physiol Plant Mol Biol **45:** 527–544

Stearns T, Hoyt MA, Botstein D (1990) Yeast mutants sensitive to antimicrotubule drugs define three genes that affect microtubule function. Genetics **124:** 251–262

Steinborn K, Maulbetsch C, Priester B, Trautmann S, Pacher T, Geiges B, Küttner F, Lepiniec L, Stierhof YD, Schwarz H, et al (2002) The Arabidopsis PILZ group genes encode tubulin-folding cofactor orthologs required for cell division but not cell growth. Genes Dev **16:** 959–971

Stoppin-Mellet V, Gaillard J, Vantard M (2006) Katanin's severing activity favors bundling of cortical microtubules in plants. Plant J **46:** 1009–1017

Sugimoto K, Williamson RE, Wasteneys GO (2000) New techniques enable comparative analysis of microtubule orientation, wall texture, and growth rate in intact roots of Arabidopsis. Plant Physiol **124:** 1493–1506

Sugimoto K, Williamson RE, Wasteneys GO (2001) Wall architecture in the cellulose-deficient rsw1 mutant of *Arabidopsis thaliana*: microfibrils but not microtubules lose their transverse alignment before microfibrils become unrecognizable in the mitotic and elongation zones of roots. Protoplasma **215:** 172–183

Thitamadee S, Tuchihara K, Hashimoto T (2002) Microtubule basis for left-handed helical growth in Arabidopsis. Nature **417:** 193–196

Tian G, Huang Y, Rommelaere H, Vandekerckhove J, Ampe C, Cowan NJ (1996) Pathway leading to correctly folded beta-tubulin. Cell **86:** 287–296

Updegraff DM (1969) Semimicro determination of cellulose in biological materials. Anal Biochem **32:** 420–424

Wang X, Zhu L, Liu B, Wang C, Jin L, Zhao Q, Yuan M (2007) *Arabidopsis* MICROTUBULE-ASSOCIATED PROTEIN18 functions in directional cell growth by destabilizing cortical microtubules. Plant Cell **19:** 877–89

Wasteneys GO (2002) Microtubule organization in the green kingdom: chaos or self-order? J Cell Sci **115:** 1345–1354

Whittington AT, Vugrek O, Wei KJ, Hasenbein NG, Sugimoto K, Rashbrooke MC, Wasteneys GO (2001) MOR1 is essential for organizing cortical microtubules in plants. Nature **411:** 610–613

Yoneda A, Higaki T, Kutsuna N, Kondo Y, Osada H, Hasezawa S, Matsui M (2007) Chemical genetic screening identifies a novel inhibitor of parallel alignment of cortical microtubules and cellulose microfibrils. Plant Cell Physiol **48:** 1393–1403